American Journal of Pathology, Vol. 150, No. 2, February 1997
Copyright © American Society for Investigative Pathology

Short Communication

Presenilin-1-Immunoreactive Neurons Are Preserved in Late-Onset Alzheimer's Disease

Panteleimon Giannakopoulos,* Constantin Bouras,*† Enikö Kövari,* Junichi Shioi,‡ Nikolaos Tezapsidis,‡ Patrick R. Hof,†§‖ and Nikolaos K. Robakis‡

From the Department of Psychiatry, HUG Belle-Idée, University of Geneva School of Medicine, Geneva, Switzerland; the Fishberg Research Center for Neurobiology and Laboratories of Neurobiology of Aging,† and the Departments of Psychiatry,‡ Geriatrics and Adult Development,§ and Ophthalmology,‖ Mount Sinai School of Medicine, New York, New York*

Recent studies have suggested that missense mutations in the presenilin-1 gene are causally related to the majority of familial early-onset Alzheimer's disease (AD). To examine the possible involvement of presenilin-1 in late-onset sporadic AD, a quantitative analysis of its distribution in the cerebral cortex of nondemented and AD patients was performed using immunocytochemistry. Stereological analyses revealed that AD brains showed a marked neuronal loss in the CA1 field of the hippocampus and hilus of the dentate gyrus, subiculum, and entorhinal cortex. In these areas, however, the fraction of neurofibrillary tangle (NFT)-free neurons showing presenilin-1 immunoreactivity was increased compared with nondemented controls. In contrast, cortical areas, which displayed no neuronal loss, did not show any significant increase in the fraction of presenilin-1-positive neurons. Moreover, presenilin-1 immunoreactivity was reduced in NFT-containing neurons. Thus, in AD, the fraction of NFT-free neurons that contained presenilin-1 varied from 0.48 to 0.77, whereas the fraction of NFT-containing neurons that were presenilin-1 positive varied from 0.1 to 0.24. Together, these observations indicate that presenilin-1 may have a neuroprotective role and that in AD low cellular expression of this protein may be associated with increased neuronal loss and NFT formation. (Am J Pathol 1997, 150:429–436)

Alzheimer's disease (AD) is a neurodegenerative disorder characterized clinically by a progressive deterioration of cognitive functions and neuropathologically by the accumulation of neurofibrillary tangles (NFTs) and senile plaques (SPs) and by the presence of neuronal and synaptic loss within the cerebral cortex.[1–6] Recently, genetic linkage studies have demonstrated that mutations in the presenilin-1 (PS-1) gene on chromosome 14q24.3 may cause 70 to 80% of early-onset familial AD cases, and to date, more than 24 missense mutations have been identified in the PS-1 gene in 40 families from various ethnic backgrounds.[7–10] No mutations have been found thus far in late-onset sporadic AD cases,[11,12] and a genetic association between variation in an intronic polymorphism located at the 3′ side of exon 9 and this common form of AD is controversial.[13–15] Furthermore, alternatively spliced PS-1 transcripts encoding truncated isoforms lacking specific transmembrane domains have been detected in both early-onset familial and late-onset sporadic AD cases.[11] Although PS-1 mRNAs have been found in many different tissues and cell types,[7,16–18] PS-1 antigens have been demonstrated by immunocytochemistry mainly in neuronal cells of all brain regions and by Western blots in neuronal cell cultures.[19–23] In neu-

Supported by grant 31–45960.95 from the Swiss National Science Foundation, Bern, Switzerland (C. Bouras and P. Giannakopoulos), grants AG05138 (P. R. Hof and N. K. Robakis) and AG08200 (N. K. Robakis) from the National Institutes of Health, Bethesda, MD, and by the A. P. Slaner family (N. K. Robakis).

Accepted for publication October 24, 1996.

Address reprint requests to Dr. Constantin Bouras, Division of Neuropsychiatry, HUG Belle-Idée, 2 chemin du Petit Bel-Air, CH-1225 Geneva, Switzerland.

rons, PS-1 seems to be preferentially concentrated in dendrites and cell bodies compared with axons.[19,20,22,23] Fractionation of brain tissue has shown that almost all of the PS-1 antigens are bound to membranes,[19] in agreement with the hydrophobic nature of the protein predicted from its amino acid sequence.[7] Moreover, PS-1 was detected in NFT-containing neurons and SPs from sporadic AD cases.[20,23,24] We have previously reported a significant decrease in the expression of PS-1 in NFT-containing neurons and proposed that low levels of this protein may be associated with an increased neuronal vulnerability.[20] To explore this hypothesis further, we quantified the distribution of PS-1 in several cortical areas of nondemented (ND) and late-onset sporadic AD cases. Our results show that PS-1-expressing neurons are spared in late-onset AD.

Materials and Methods

A total of 26 patients (16 women, 81.2 ± 2.4 years old, and 10 men, 79.5 ± 2.0 years old), who died and were autopsied in the Hospitals of the University of Geneva School of Medicine, were included in the present study. Among them, 14 patients (9 women, 80.5 ± 1.8 years old, and 5 men, 78.8 ± 1.7 years old) had no signs of cognitive impairment. Most of these patients were admitted to the hospital with symptoms of cardiac failure, pulmonary insufficiency, or chronic vascular disease. Their mean Mini-Mental State Examination score at the final admission was 29.0 ± 1.0,[25] and the score of the extended Clinical Dementia Rating Scale[26] applied retrospectively was 0.6 ± 0.2. These nondemented patients form the ND group of the present study. The clinical diagnosis was confirmed neuropathologically by the absence of significant histopathological changes in the ND group. The remaining 12 patients (7 women, 82.5 ± 2.6 years old, and 5 men, 80.9 ± 2.7 years old) showed severe cognitive deterioration and were classified clinically as AD according to DSM-IV criteria. Their hospitalization was motivated by the presence of major behavioral disturbances such as psychomotor agitation, feeding difficulties, marked aggressiveness, delusions of persecution, and suicidal thoughts. Detailed neuropsychological evaluation performed at least twice during the 6 months before death revealed a significant decline of higher cortical functions characterized by severe memory impairment, temporal and spatial disorientation, language impoverishment, apraxia, and agnosia in all of the cases. These demented patients form the AD group of this study. The mean Mini-Mental State Examination score of this group was 19.5 ± 2.5, and the extended Clinical Dementia Rating score was 3.5 ± 0.5. The neuropathological investigation according to the Consortium to Establish a Registry for Alzheimer's disease criteria[27] confirmed the clinical diagnosis of AD.

All of the brains were obtained within a short postmortem delay (2 to 8 hours) and were fixed overnight in 4% paraformaldehyde. After macroscopic examination, tissue blocks were dissected from the hippocampal formation, including the entorhinal, inferior temporal, and superior frontal cortex, and postfixed for 48 to 72 hours in 4% paraformaldehyde. For microscopic purposes, blocks were washed in a series of graded sucrose solutions (12, 16, 18, and 30%) in cold phosphate-buffered saline (PBS), frozen, and cut at 12-μm-thick sections. For routine neuropathological evaluation, tissues were stained with Nissl, hematoxylin and eosin, and Globus silver impregnation stains.[28] PS-1 expression was detected using an affinity-purified polyclonal antibody raised against the human long isoform PS-1 sequence 311 to 330.[19] Full characterization of this antibody, including Western blot confirmation of its specificity in human and rodent brain, as well as in neuronal and glial cell lines, has been previously reported.[19] In the present study, specificity of staining was confirmed by preabsorption with the corresponding synthetic peptide. The percentages of PS-1-immunoreactive NFT-free neurons were obtained from Nissl-stained sections. Briefly, 12-μm-thick cryostat sections were rinsed in PBS followed by treatment for 10 minutes with potassium permanganate (0.25%) to mask lipofuscin fluorescence.[28] After rinsing in PBS, slides were treated with 1% oxalic acid and 1% potassium metabisulfite in PBS for 2 minutes. After incubation overnight with the primary anti-PS-1 antibody, sections were incubated with a peroxidase-conjugated anti-rabbit secondary antibody for 1 hour followed by rinsing with PBS. The sections were treated with 3,3′-diaminobenzidine as a chromogen and counterstained with Nissl stain. In addition to staining with PS-1, double labeling was performed in adjacent sections with a modified thioflavin S stain to visualize NFTs and SPs in AD cases.[28]

To assess whether the anti-PS-1 antibody cross-reacts with lipofuscin, two additional experiments were performed. First, 12-μm-thick cryostat sections from the hippocampal formation and frontal cortex of a 6-month-old child were stained as described above. Second, a series of 10 randomly selected, untreated sections from all ND and AD cases were examined for lipofuscin autofluorescence, and the pattern of lipofuscin distribution was compared with

that of PS-1 in each case in immediately adjacent sections stained with the anti-PS-1 antibody.

In all of the brains, total and PS-1-immunoreactive neuron densities were estimated in the anterior CA1 to CA3 fields of the hippocampus and hilus of the dentate gyrus, subiculum, layers II and V of the entorhinal cortex, and layers II-III and V-VI of areas 9 (superior frontal cortex) and 20 (inferior temporal cortex) by light microscopy. In addition, the total and PS-1-immunoreactive number of NFT-containing neurons and SPs was determined in all of these areas in AD cases using a combination of light and fluorescence microscopy. Detection of NFT-containing neurons and SPs was made using the fluorescence microscopy settings, whereas PS-1 immunoreactivity was examined after occluding the fluorescence light path, removing fluorescence filters, and turning on the conventional bright light for each counting frame. Neuron densities per cubic millimeter were estimated using the optical disector, an unbiased stereological counting method allowing all regions within the structure of interest an equal chance of being analyzed; ie, there is no bias in sampling and counts do not depend on variables such as the size and shape of neurons.[3,4,29,30] The technique relies on a three-dimensional counting box located entirely within the tissue section, and objects are quantified by focusing in the section depth (ie, in the *z* axis). The fact that the three-dimensional counting box is located within the thickness of the section and the existence of exclusion (forbidden) planes guarantee that any neuron may be counted only once.[3,4,29,30] Total neuron and NFT numbers were not obtained in the present study because only the anterior portion of the hippocampus and only topographically equivalent samples of areas 9 and 20 were available for analysis. The volume of these samples was variable, rendering comparison of total cell numbers impossible from case to case. For this reason, neuron and NFT densities per cubic millimeter were assessed in a 1 in 10 series of sections, 500 μm apart, using a Zeiss 63× Plan-Neofluar objective (numerical aperture 1.4). The number of SPs was determined in each area and the mean density per square millimeter was calculated. All analyses were performed by two independent investigators with a reliability of 0.93, using a computer-assisted image analysis system consisting of a Zeiss Axioplan microscope, a high-sensitivity LH-4036 camera (LHESA Electronic), a COMPAQ Deskpro 386/20 microcomputer, and a SAMBA 2005 software system developed by TITN (ALCATEL, Grenoble, France).

The percentages of PS-1-immunoreactive neurons in ND cases as well as the percentages of PS-1-immunoreactive NFT-free and NFT-containing neurons and SPs in AD cases were evaluated within each cortical layer for each selected area. Statistical differences in the prevalence of PS-1-containing neurons between the two diagnosis groups and between NFT-free and NFT-containing neurons in AD cases were assessed by one-way analysis of variance.

Results

In both ND and AD brains, PS-1 labeling was intensely concentrated in the cytoplasm of neurons as well as in the proximal segments of basal and apical dendrites (Figure 1a). No PS-1 immunoreactivity was detected in axons. Scarce glial cells were also PS-1 positive, but their number was very low in both ND and AD brains (Figure 1a). The anti-PS-1 antibody used in the present study did not cross-react with lipofuscin. In fact, the distribution of PS-1 in the 6-month-old case was comparable to that observed in our ND cases (Figure 1, a and b). In addition, no co-localization was found between lipofuscin autofluorescence and PS-1 staining (data not shown). No immunostaining was observed when the primary anti-PS-1 antibody was omitted.

Consistent with previous data,[3,5] stereological estimates of Nissl-stained neuronal densities demonstrated that AD cases had consistently lower neuron densities in the CA1 field and hilus of the dentate gyrus, subiculum, and layers II-III and V-VI of the entorhinal cortex than ND brains (Table 1). Despite the neuronal loss, the number of neurons showing PS-1 immunoreactivity in these areas in all AD cases was comparable to that found in ND cases. In the other cortical areas, Nissl-stained and PS-1-containing neuron densities did not significantly differ between the ND and AD brains (Table 1).

As counting of PS-1-immunoreactive neurons in AD includes both NFT-free and NFT-containing neurons, double labeling was performed to differentiate these two neuronal subpopulations (Figure 1c), and the percentage of PS-1-containing neurons was calculated (Table 2). In the ND group, the prevalence of neurons showing PS-1 immunoreactivity varied from 32 to 58%, depending on the area. The CA1 field had the lowest percentage of PS-1-immunoreactive neurons, whereas in the CA2 to CA3 fields and hilus of the dentate gyrus as well as in layers II-III of areas 9 and 20, at least 50% of all neurons were PS-1 immunoreactive. In AD, the percentage of NFT-free neu-

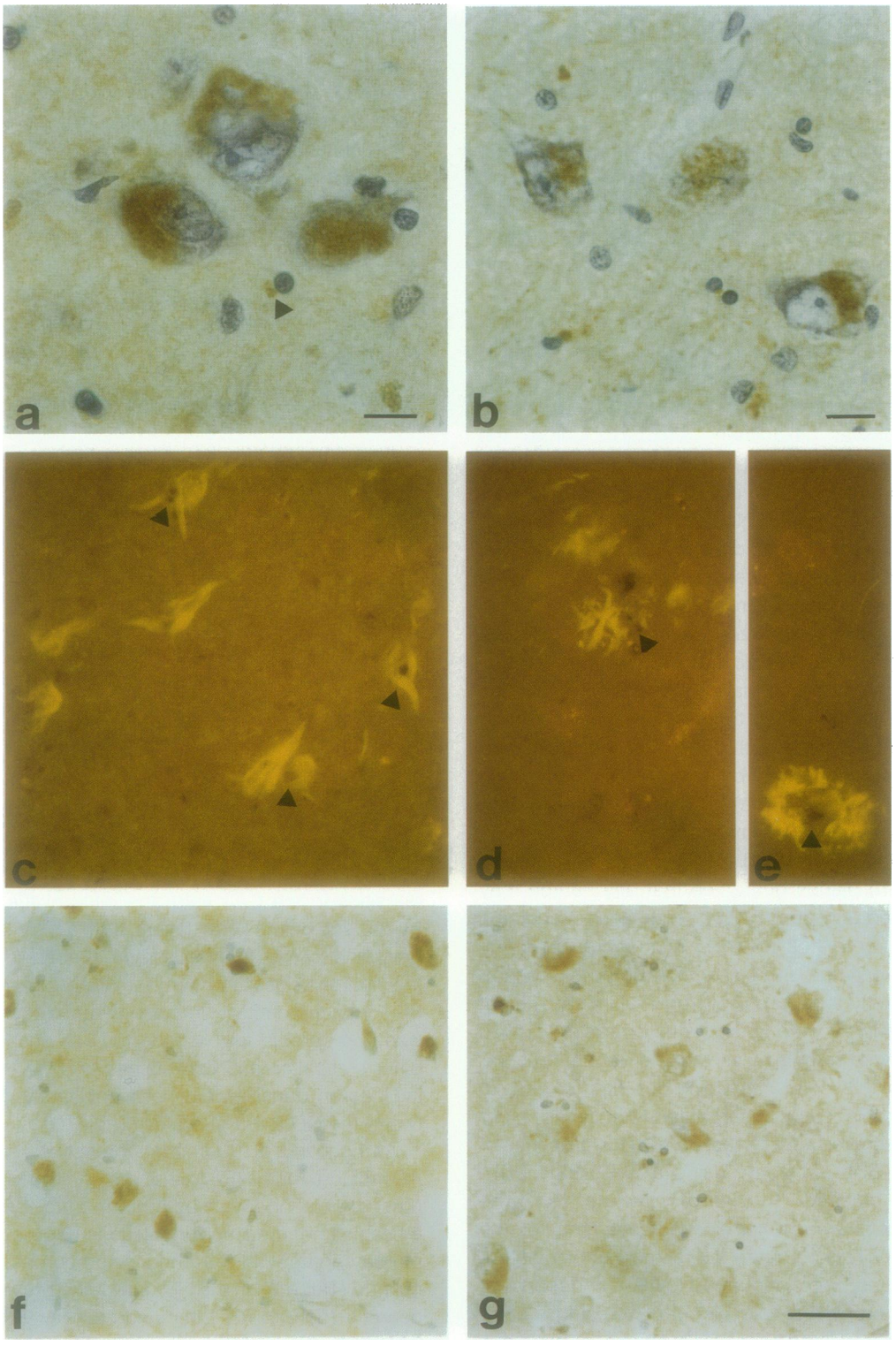

Figure 1. a *and* b: *Immunocytochemical visualization of NFT-free neurons containing PS-1 in the CA1 field in a nondemented 80-year-old ND patient* (a) *and in a 6-month-old child* (b). *A thick perinuclear PS-1 staining was observed in pyramidal neurons in both cases.* c *to* e: *Double-labeling visualization of PS-1-immunoreactive NFT-containing neurons* (c) *and SPs* (d *and* e) *in the entorhinal cortex in an 81-year-old patient with AD. Note the presence of PS-1 immunoreactivity in both degenerating neurites* (d) *and amyloid core* (e) *in SPs.* f *and* g: *PS-1-immunoreactive neurons in the subiculum in a nondemented 83-year-old patient* (f) *and in an 84-year-old patient with AD* (g). *Note the presence of higher PS-1-immunoreactive neuron densities in the AD patient. Visualization of neurons containing PS-1 was made using an antibody against the PS-1 in Nissl-counterstained sections* (a, b, f, g). *Double labeling with modified thioflavin S stain was performed to visualize PS-1-immunoreactive NFT-containing neurons* (c) *and SPs* (d *and* e). Arrows *indicate PS-1 staining in a glial cell* (a), *in NFT-containing neurons* (c), *and in SPs* (d *and* e). *Scale bars, 5 μm* (a *to* e) *and 20 μm* (f *and* g).

Table 1. *Neuron Densities in ND and AD Cases*

Area/layer	Niss1-stained neurons		PS-1-immunoreactive neurons	
	ND	AD	ND	AD
CA1	28832 ± 3261	18980 ± 1843*	9169 ± 1076	10250 ± 996
CA2-3	43072 ± 3482	35680 ± 2427	22268 ± 1754	19980 ± 1182
Hilus	25290 ± 2234	13570 ± 2795†	13907 ± 1229	10178 ± 1046
Subiculum	32860 ± 2783	22170 ± 2180*	14458 ± 1225	17293 ± 1700
Entorhinal II	39580 ± 2425	28210 ± 2321*	20185 ± 1237	21539 ± 1764
Entorhinal V	63640 ± 3410	25490 ± 1614‡	20728 ± 1398	16316 ± 1094
20 II-III	28810 ± 1319	22220 ± 1177	14693 ± 973	13109 ± 894
V-VI	26880 ± 2158	23310 ± 2589	11289 ± 907	11188 ± 1243
9 II-III	32240 ± 1663	32060 ± 3012	19021 ± 1023	20518 ± 1928
V-VI	33010 ± 2435	29710 ± 1949	15845 ± 1169	16043 ± 1053

Results represent neuron number/mm^3 (±SEM) in each area. These densities were estimated using the optical disector method.[3,4,28,29] Note that a statistically significant neuronal loss is observed in the CA1 field and hilus of the dentate gyrus, subiculum, and layers II and V of the entorhinal cortex in AD cases compared with ND cases. Note also the relative preservation of PS-1-immunoreactive neurons in these areas. Cortical layers are indicated by Roman numerals. Statistical analysis was performed by one-way analysis of variance.

*$P < 0.05$ compared with ND.

†$P < 0.01$ compared with ND.

‡$P < 0.001$ compared with ND.

rons that were PS-1 positive was increased and varied from 47 to 77%, depending on the cortical area. This increase was statistically significant in the CA1 field and hilus of the dentate gyrus, subiculum, and layers II-III and V-VI of the entorhinal cortex (Table 2). Importantly, these areas also displayed a substantial neuronal loss in all AD cases (Table 1). For example, the percentages of NFT-free neurons showing PS-1 immunoreactivity in the CA1 field, subiculum, and layer V of the entorhinal cortex were 56, 74, and 66%, respectively. In the corresponding areas of control brains, the percentages of PS-1-positive neurons were 32, 42, and 41%, respectively (Figure 1, f and g; Table 2).

In all AD cases, high NFT densities (>1000/mm^3) were observed in the CA1 field, layers II and V of the entorhinal cortex, and layers II-III and V-VI of area 20. In the subiculum, there was moderate NFT formation (500 to 1000/mm^3), whereas the hilus of the dentate gyrus and layers II-III and V-VI of area 9 displayed very low NFT densities (<250/mm^3) in all of the cases. Only a few NFT-containing neurons displayed PS-1 labeling in the areas studied. For example, the percentages of PS-1-positive NFT-containing neurons were 10 to 20% in hippocampal subdivisions and 13 to 24% in neocortical areas. These percentages were significantly lower than those of the NFT-free neurons in all of the cortical areas of AD brains (Table 2).

In most SPs, PS-1 immunoreactivity was concentrated in the amyloid core (Figure 1e). However, in a small number of SPs, PS-1 labeling was observed in neurites in the vicinity of the amyloid core (Figure 1d). There was a marked variability of the number of PS-1-labeled SPs within the cerebral cortex. For instance, 20 to 30% of SPs were PS-1 immunoreactive

Table 2. *Prevalence in ND and AD Cases*

Area/layer	ND, % NFT-free neurons	AD		
		% NFT-free neurons	% NFT-containing neurons	SP
CA1	31.8 ± 4.7	55.6 ± 3.6*	10.2 ± 3.7†	29.1 ± 5.6
CA2-3	51.7 ± 2.6	54.3 ± 6.4	16.0 ± 2.2†	21.1 ± 0.8
Hilus	52.0 ± 3.3	75.8 ± 2.4*	22.2 ± 1.7†	57.8 ± 4.3
Subiculum	41.4 ± 5.4	74.0 ± 3.6‡	19.6 ± 1.8†	23.8 ± 3.8
Entorhinal II	48.9 ± 5.1	77.1 ± 3.7*	21.7 ± 4.8†	19.2 ± 3.3
Entorhinal V	40.6 ± 3.7	65.9 ± 2.8‡	21.3 ± 5.6†	23.6 ± 2.8
20 II-III	50.3 ± 3.4	58.9 ± 5.8	11.0 ± 2.7†	47.2 ± 4.9
V-VI	40.2 ± 4.2	47.7 ± 5.1	24.4 ± 4.6§	52.8 ± 2.8
9 II-III	58.4 ± 2.5	64.1 ± 5.7	18.7 ± 2.7†	47.3 ± 5.8
V-VI	47.9 ± 2.6	54.4 ± 4.9	12.6 ± 2.2†	39.8 ± 2.1

Results represent the percentages of PS-1-immunoreactive NFT-free and NFT-containing neurons and SP in each area. Note that AD cases displayed significantly higher PS-1 prevalence in NFT-free neurons only in areas that show significant neuronal loss (see Table 1). In AD cases, PS-1 prevalence was significantly lower in NFT-containing compared with NFT-free neurons. Cortical layers are indicated by Roman numerals. Statistical analysis was performed by one-way analysis of variance.

*$P < 0.005$; ‡$P < 0.001$ compared with the percentage of NFT-free neurons showing PS-1 immunoreactivity in ND cases.

§$P < 0.005$; †$P < 0.001$ compared with the percentage of NFT-free neurons showing PS-1 immunoreactivity in AD cases.

in the CA1 field, subiculum, and entorhinal cortex, whereas this percentage was 58% in the hilus of the dentate gyrus, 53% in layers V-VI of area 20, and 47% in layers II-III of areas 9 and 20 (Table 2).

Discussion

The present data indicate that PS-1-immunoreactive neurons are well preserved in late-onset sporadic AD, suggesting that the lack of PS-1 expression may be related to both neuronal loss and NFT formation in the course of this disorder. Several studies in mouse and human brain have shown that PS-1 is widely distributed in the cerebral cortex, where it is mainly expressed in the cytoplasm of neurons.[19–23] Our findings confirm these observations and demonstrate that the regional distribution of PS-1 does not differ in ND and AD cases.[23] However, the quantitative analysis revealed that in AD there was a relative increase in the number of NFT-free neurons containing PS-1 in all cortical areas compared with the ND cases. It could be argued that PS-1 overexpression may take place in preserved neuronal subpopulations in AD. However, the increase in PS-1 immunoreactivity was statistically significant only in areas showing a marked neuronal loss such as the CA1 field and hilus of the dentate gyrus, subiculum, and entorhinal cortex,[3,4] indicating that this increase is mainly due to the relative depletion in PS-1-negative neurons. Altogether, these findings suggest that PS-1 may have a neuroprotective role and that neuronal populations that express low levels of this protein may show a higher vulnerability in the course of the degenerative process.[20] This notion is supported by the low percentage of the NFT-containing neurons that were PS-1 immunoreactive in both the hippocampal formation and neocortex of all AD cases examined. Recently, Uchihara et al[23] examined the cellular distribution of PS-1 in sporadic AD cases and reported that NFT-containing neurons do not exhibit an intense PS-like immunoreactivity, although no quantitative data were included in this study. Similarly, double labeling for PS-2 gene expression and paired helical filament immunoreactivity revealed that only a small subset of neurons expressing PS-2 co-localized with paired helical filament formation.[31] Our results extend these observations in that they show that less than 25% of NFT-containing neurons are PS-1 positive in AD. Such a conclusion must be drawn with caution for the present study as it is possible that the absence of PS-1 staining in NFT-containing neurons may be partly due to the displacement of PS-1-containing organelles by NFT formation in the cytoplasm.

The staining of SP with our antibody that is specific for PS-1 residues 311 to 330 is in agreement with recent reports that a carboxyl-terminal fragment of PS-1 may be a component of AD amyloid.[23,24] Although in most SPs PS-1 immunoreactivity appears to be located in the amyloid core, PS-1-labeled degenerating neurites were also visualized in a few SPs. Moreover, our data show that the percentage of PS-1-immunoreactive SPs varies between 20 and 50%, depending on the cortical area, and that this variation does not correlate with the severity of the neuronal loss. The exact significance of the association of PS-1 staining with SPs is therefore unclear. However, a large number of proteins have been detected in association with SPs, and it is likely that some of these proteins are adsorbed nonspecifically on to the amyloid fibers when released as a result of nerve cell death and lysis.[32]

The biological functions of PS-1 are not yet elucidated, although its structure suggests that it may function as a receptor or ion channel.[7] Recently, Vito et al[33] revealed a striking homology between the PS-2 gene and an apoptosis-related gene, ALG-3, and proposed that PS genes might confer resistance to apoptotic cell death in AD. Although it is well established that neuronal loss related to NFT formation is the rule in AD,[5] this and previous studies indicate that there is substantial neuronal loss in areas usually spared by NFTs such as the hilus of the dentate gyrus.[3,4] It is thus possible that high PS expression protects against both NFT-related and NFT-unrelated neuronal loss. In agreement with a recent immunocytochemical study,[23] our results in NFT-free and NFT-containing neurons strengthen this hypothesis and stress the necessity of additional molecular genetic and biochemical analyses to clarify this issue.

Acknowledgments

We thank M. Surini and P. Y. Vallon for expert technical assistance.

References

1. Bouras C, Hof PR, Giannakopoulos P, Michel JP, Morrison JH: Regional distribution of neurofibrillary tangles and senile plaques in the cerebral cortex of elderly patients: a quantitative evaluation of a one-year autopsy population from a geriatric hospital. Cereb Cortex 1994, 4:138–150
2. Braak H, Braak E: Neuropathological stageing of

Alzheimer-related changes. Acta Neuropathol 1991, 82:239–259
3. West MJ, Coleman PD, Flood DG, Troncoso JD: Differences in the pattern of hippocampal neuronal loss in normal aging and Alzheimer's disease. Lancet 1994, 344:769–772
4. West MJ: Regionally specific loss of neurons in the aging human hippocampus. Neurobiol Aging 1993, 14: 287–293
5. Gómez-Isla T, Price JL, McKeel DW Jr, Morris JC, Growdon JH, Hyman BT. Profound loss of layer II entorhinal cortex neurons occurs in very mild Alzheimer's disease. J Neurosci 1996;16:4491–500
6. Masliah E, Ellisman M, Carragher B, Mallory M, Young S, Hansen L, DeTeresa R, Terry RD: Three-dimensional analysis of the relationship between synaptic pathology and neuropil threads in Alzheimer's disease. J Neuropathol Exp Neurol 1992, 51:404–414
7. Sherrington R, Rogaev EI, Liang Y, Rogaeva EA, Levesque G, Ikeda M, Chi H, Lin C, Li G, Holman K, Tsuda T, Mar L, Foncin JF, Bruni AC, Montesi MP, Sorbi S, Rainero I, Pinessi L, Nee L, Chumakov I, Pollen D, Brookes A, Sanseau P, Polinsky RJ, Wasco W, DaSilva HAR, Haines JL, Pericak-Vance MA, Tanzi RE, Roses AD, Fraser PE, Rommens JM, St George-Hyslop PH: Cloning of a gene bearing missense mutations in early-onset familial Alzheimer's disease. Nature 1995, 375: 754–760
8. Cruts M, Backhovens H, Wang SY, Van Gassen G, Theuns J, De Jonghe C, Wehnert A, De Voecht J, De Winter G, Cras P, Bruyland M, Datson N, Weissenbach J, Dunnen JT, Martin J, Hendriks L, Van Broeckhoven C: Molecular genetic analysis of familial early-onset Alzheimer's disease linked to chromosome 14q24.3. Hum Mol Genet 1995, 4:2363–2371
9. Campion D, Brice A, Hannquin D, Tardieu S, Dubois B, Calenda A, Brun E, Penet C, Tayot J, Martinez M, Bellis M, Mallet J, Agid Y, Clerget-Darpoux F: Mutations of the presenilin I gene in families with early-onset Alzheimer's disease. Hum Mol Genet 1995, 4:2373–2377
10. Clark RF, Hutton M, Fuldner R, Froelich S, Karran E, Talbot C, Crook R, Lendon C, Prihar G, He C, Korenblat K, Martinez A, Wragg M, Busfield F, Behrens MI, Myers A, Norton J, Morris J, Mehta N, Pearson C, Lincoln S, Baker M, Duff K, Zehr C, Perez-Tur J, Houlden H, Ruiz A, Ossa J, Lopera F, Arcos M, Madrigal L, Collinge J, Humphreys C, Ashworth A, Sarner S, Fox N, Harvey R, Kennedy A, Roques P, Cline RT, Phillips CA, Venter JC, Forsell L, Axelman K, Lilius L, Johnston J, Cowburn R, Vitanen M, Winblad B, Kosik K, Haltia M, Poyhonen M, Dickson D, Mann D, Neary D, Snowden J, Lantos P, Lannfelt L, Rossor M, Roberts GW, Adams MD, Hardy J, Goate A: The structure of the chromosome 14 Alzheimer's disease gene, presenilin 1 (PS-1), and identification of six novel mutations in early onset AD families. Nature Genet 1995, 11:219–222
11. Anwar R, Moynihan TP, Ardley H, Brindle N, Coletta PL, Cairns N, Markham AF, Robinson PA: Molecular analysis of the presenilin 1 (S182) gene in "sporadic" cases of Alzheimer's disease: identification and characterization of unusual splice variants. J Neurochem 1996, 66:1774–1777
12. Tsuda T, Chi H, Liang Y, Rogaeva EA, Sherrington R, Levesque G, Ikeda M, Rogaev EI, Pollen D, Freedman M, Duara R, St George-Hyslop PH: Failure to detect missense mutations in the S182 gene in a series of late-onset Alzheimer's disease cases. Neurosci Lett 1995, 201:188–190
13. Wragg M, Hutton M, Talbot C, Busfield F, Han SW, Lendon C, Clark RF, Morris JC, Edwards D, Goate A, Pfeiffer E, Crook R, Prihar G, Phillips H, Baker M, Hardy J, Rossor M, Houlden H, Karran E, Roberts G, Craddock N: Genetic association between intronic polymorphism in presenilin-1 gene and late-onset Alzheimer's disease. Lancet 1996, 347:509–512
14. Pérez-Tur J, Warrant-De Vrieze F, Lambert JC, Chartier-Harlin MC and the Alzheimer Study Group: presenilin-1 polymorphism and Alzheimer's disease. Lancet 1996, 347:1560–1561
15. Scott WK, Growdon JH, Roses AD, Haines JL, Pericak-Vance MA: Presenilin-1 polymorphism and Alzheimer's disease. Lancet 1996, 347:1187
16. Kovacs DM, Fausett HJ, Page KJ, Kim TW, Moir RD, Merriam DE, Hollister RD, Hallmark OG, Mancini R, Felsenstein KM, Hyman BT, Tanzi RE, Wasco W: Alzheimer-associated presenilins 1 and 2: neuronal expression in brain and localization to intracellular membranes in mammalian cells. Nature Med 1996, 2:224–229
17. Cribbs DH, Chen L, Bendle SM, LaFerla FM: Widespread neuronal expression of the presenilin-1 early-onset Alzheimer's disease in the murine brain. Am J Pathol 1996, 148:1797–1806
18. Suzuki T, Nishiyama K, Murayama S, Yamamoto A, Sato S, Kanazawa I, Sakaki Y: Regional and cellular presenilin 1 gene expression in human and rat tissues. Biochem Biophys Res Commun 1996, 219:708–713
19. Elder GA, Tezapsidis N, Carter J, Shioi J, Bouras C, Li D, Johnston JM, Efthimiopoulos S, Friedrich Jr VL, Robakis NK. Identification and neuron specific expression of the S182/presenilin I protein in human and rodent brains. J Neurosci Res 1996, 45: 308–320
20. Bouras C, Giannakopoulos P, Shioi J, Tezapsidis N, Robakis NK: Presenilin-1 polymorphism and Alzheimer's disease. Lancet 1996, 347:1185–1186
21. Moussaoui S, Czech C, Pradier L, Blanchard V, Bonici B, Gohin M, Imperato A, Revah F: Immunohistochemical analysis of presenilin-1 expression in the mouse brain. FEBS Lett 1996, 383:219–222
22. Cook DG, Sung JC, Golde TE, Felsenstein KM, Wojczyk BS, Tanzi RE, Trojanowski JQ, Lee VM-Y, Doms RW: Expression and analysis of presenilin 1 in a human neuronal system: localization in cell bodies and dendrites. Proc Natl Acad Sci USA 1996, 93:9223–9228
23. Uchihara T, El Hachimi HK, Duyckaerts C, Foncin J-F, Fraser PE, Levesque L, St George-Hyslop PH, Hauw J-J: Widespread immunoreactivity of presenilin in neu-

rons of normal and Alzheimer's disease brains: double-labeling immunohistochemical study. Acta Neuropathol 1996, 92:325–330
24. Wisniewski T, Palha JA, Ghiso J, Frangione B: S182 protein in Alzheimer's disease neuritic plaques. Lancet 1995, 346:1366
25. Folstein MF, Folstein SE, McHugh PR: Mini-Mental State: a practical method for grading the cognitive state of patients for the clinician. J Psychiatr Res 1975, 12:189–198
26. Heyman A, Wilkinson WE, Hurwitz BL, Helms MJ, Haynes CS, Utley CM, Gwyther LP: Early-onset Alzheimer's disease: clinical predictors of institutionalization and death. Neurology 1987, 37:980–984
27. Mirra SS, Heyman A, McKeel D, Sumi SM, Crain BJ, Brownlee LM, Vogel FS, Hughes JP, van Belle G, Berg L: The Consortium to Establish a Registry for Alzheimer's disease (CERAD). II. Standardization of the neuropathologic assessment of Alzheimer's disease. Neurology 1991, 41:479–486
28. Vallet PG, Guntern R, Hof PR, Golaz J, Delacourte A, Robakis NK, Bouras C: A comparative study of histological and immunohistochemical methods for neurofibrillary tangles and senile plaques in Alzheimer's disease. Acta Neuropathol 1992, 83:170–178
29. Sterio DC: The unbiased estimation of number and sizes of arbitrary particles using the disector. J Microsc 1984, 134:127–136
30. Coggeshall RE, Lekan HA: Methods for determining numbers of cells and synapses: a case for more uniform standards of review. J Comp Neurol 1996, 364: 6–15
31. Deng G, Su JH, Cotman CW: Gene expression of Alzheimer-associated presenilin-2 in the frontal cortex of Alzheimer and aged control brain. FEBS Lett 1996, 394:17–20
32. Robakis NK: β-Amyloid and amyloid precursor protein: chemistry, molecular biology, and neuropathology. Alzheimer's Disease. Edited by RD Terry, R Katzman, KL Bick. New York, Raven Press, 1994, pp 317–326
33. Vito P, Lacan E, D'Adamio L: Interfering with apoptosis: Ca^{2+}-binding protein ALG-2 and Alzheimer's disease gene ALG-3. Science 1996, 271:521–525